Ultrahigh Efficiency Fluorescent Single and Bi-Layer Organic Light Emitting Diodes: The Key Role of Triplet Fusion

7 AUTHORS, INCLUDING:

Marc Kenneth Etherington
Durham University
2 PUBLICATIONS **42** CITATIONS

SEE PROFILE

Gareth Griffiths
Durham University
6 PUBLICATIONS **151** CITATIONS

SEE PROFILE

Figen Turksoy
The Scientific & Technological Research Co…
17 PUBLICATIONS **181** CITATIONS

SEE PROFILE

Andy Monkman
Durham University
416 PUBLICATIONS **9,835** CITATIONS

SEE PROFILE

Materials Views
www.MaterialsViews.com

ADVANCED
FUNCTIONAL
MATERIALS
www.afm-journal.de

FULL PAPER

Ultrahigh Efficiency Fluorescent Single and Bi-Layer Organic Light Emitting Diodes: The Key Role of Triplet Fusion

Chien-Jung Chiang, Alpay Kimyonok, Marc K. Etherington, Gareth C. Griffiths, Vygintas Jankus, Figen Turksoy,* and Andy P. Monkman*

A new family of anthracene core, highly fluorescent emitters is synthesized which include diphenylamine hole transport end groups. Using a very simple one or two layer organic light emitting diode (OLED) structure, devices without outcoupling achieve an external quantum efficiency of 6% and photonic efficiencies of 20 cd/A. The theoretical maximum efficiency of such devices should not exceed 3.55%. Detailed photophysical characterization shows that for these anthracene based emitters $2T_1 \leq T_n$ and so in this special case, triplet fusion can achieve a singlet production yield of 0.5. Indeed, delayed electroluminescence measurements show that triplet fusion contributes 59% of all singlets produced in these devices. This demonstrates that when triplet fusion becomes very efficient, fluorescent OLEDs even with very simple structures can approach an internal singlet production yield close to the theoretical absolute maximum of 62.5% and rival phosphorescent-based OLEDs with the added advantage of much improved stability.

1. Introduction

Since their introduction into phosphorescent organic light emitting diodes (PhOLED), heavy metal based light emitting small molecules, i.e., fac-tris(2-phenylpyridine)iridium(III) (Ir(ppy)₃)[1] and bis(2-(2′-benzo[4,5-a]thienyl)pyridinato-N,C³′) iridium(acetylacetonate) [Btp₂Ir(acac)],[2] where highly efficient phosphorescence arising from the strong spin-orbit coupling in these emitters, which utilizes up to 100% of excitons generated in the device.[3] They have become the most promising emitters for the commercialization of OLED devices in the past decade. By optimizing the ratio of the phosphorescent dopant to the host material, the usually elaborately-structured PhOLEDs can now reach efficiencies of 75 lm/W for green,[4] 17 lm/W for red,[5] and 48 lm/W for blue,[6] at the brightness of 100 cd/m². With efficient outcoupling and optimized whole device architecture, green PhOLEDs attaining 187 lm/W have been reported.[7] However, loss of energy from the injected electron-hole pair in forming the triplet exciton lowers the overall power efficiency of the devices and also there are general problems with the lifetime stability of the heavy metal complexes, especially blue emitters.[8] The fact that the phosphorescent OLED device relies on a host-dopant system also makes it more difficult to find a host material that has higher triplet energy than the emitting complex, to be used in the deep-blue emission system.[9]

However, it is generally believed that the upper limit of the external quantum efficiency (EQE) of fluorescent OLEDs is 5% due to the following equation:

$$\text{EQE}_{max} = \eta_{op} \times \phi_{fl} \times \eta_r \times \gamma \approx 0.2 \times 1 \times 0.25 \times 1 = 5\% \quad (1)$$

where η_{op} is the optical out coupling factor, Φ_{fl} is the fluorescence quantum yield, η_r is the possibility that an exciton is formed as a singlet and finally γ is the charge balance factor. Kondakov et al.[10] have recently reported OLEDs, having a total thickness of ≈200 nm, with a 6 layered (excluding cathode and anode) device architecture including a fluorescent dopant species, having an EQE of 11.1% where >50% of the fluorescence was identified as delayed florescence contributed from triplet fusion (TF).[11,12] Even if the optical out coupling factor was underestimated by Kondakov et al.,[7] the rate of singlet exciton formation is still surely larger than 25%. Furthermore, King et al.[13] have also shown that in a polymer based OLED, high EQE can be attributed to a large TF contribution to the overall singlet production yield. Therefore, a new fluorescent OLED structure can be envisaged by confining the long-lifetime triplet excitons in an energy well which is deep enough to form a dense triplet exciton pool and therefore enhance the rate of TF to maximize regeneration of singlet excitons contributing to the electroluminescence.

Dr. C.-J. Chiang, M. K. Etherington, G. C. Griffiths,
Dr. V. Jankus, Prof. A. P. Monkman
Institute of Photonic Materials
Department of Physics
Durham University
South Road, Durham, DH1 3LE, UK
E-mail: a.p.monkman@durham.ac.uk;
Dr. A. Kimyonok, Dr. F. Turksoy
TUBITAK Marmara Research Center
Chemistry Institute
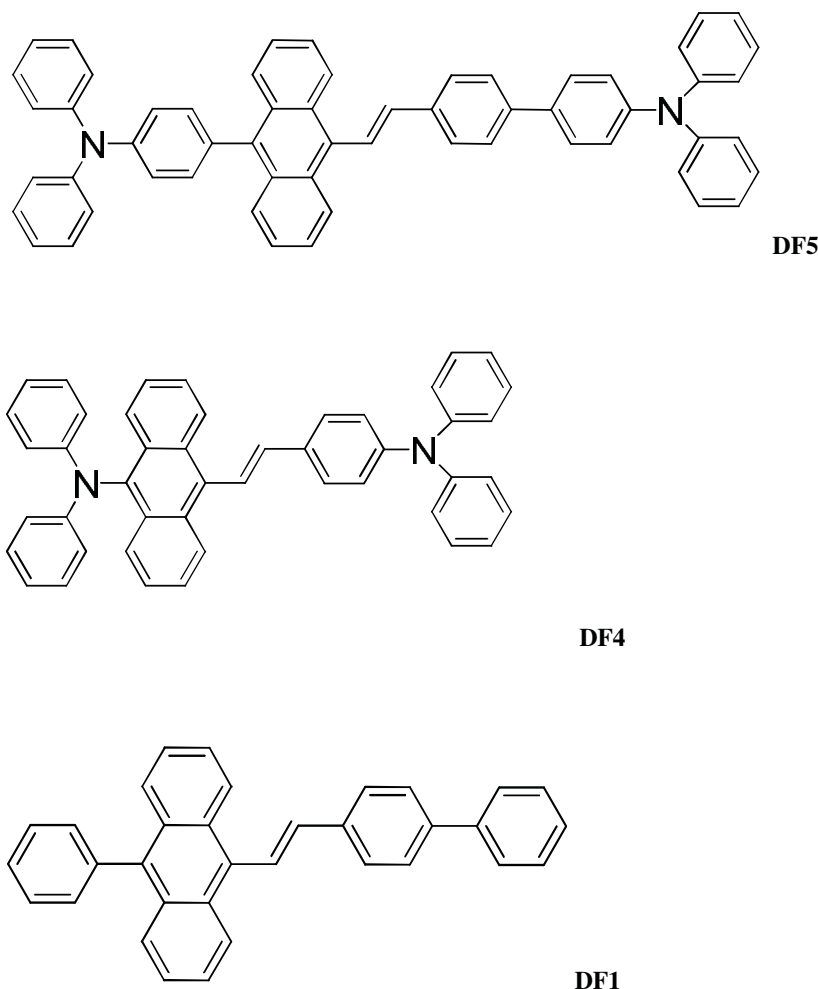P.O. Box 21, Gebze 41470 Kocaeli, Turkey
E-mail: figen.tursoy@tubitak.gov.

FULL PAPER

DF5

DF4

DF1

Figure 1. Molecular structure of the new anthracene core emitters investigated in this study.

since the 1960s.[14] Strong DF was therefore expected to be observed when using these new materials as the emitters in the OLED system. The lowest unoccupied molecular orbital (LUMO), highest occupied molecular orbital (HOMO) and the triplet energy levels of these new emitters are summarized in Table S1 in the Supporting Information. The electron transporting material 1,3,5-tri(1-phenyl-1H-benzo[d]imidazol-2-yl)phenyl (TPBi)[15] has been used as the host material because of its large triplet energy and energy matching HOMO and LUMO as shown in Table S1 in the Supporting Information. The ≈1 eV energy barrier between the triplet energy of the host and emitters prevents the triplet excitons formed on the dopant from transferring back to the host allowing TF to occur efficiently within the high density of triplets. Devices made from these emitters show efficiencies far in excess of the 25% singlet generation limit, having a very high DF contribution. This is explained by the high efficiency of triplet fusion in these emitters. In all cases the devices also have very simple structures with only one or two active layers.

2. Results

For the basic characterization of these DF emitters, measurements of their quantum yields, singlet lifetimes and the decay profiles of their phosphorescence (PH) and delayed-fluorescence (DF) were measured in films of the emitter isolate in zeonex, drop cast films.

Figure 2a shows the absorption of **DF4** and **DF5** in a zeonex host, and Figure 2b shows the emission of the films. All emitters have strong absorption at a wavelength of 300 nm and absorption at longer wavelengths of 410 and 450 nm respectively, which indicates that **DF5** has the longer conjugated chain as expected. Extinction coefficients of **DF4** and **DF5** dissolved
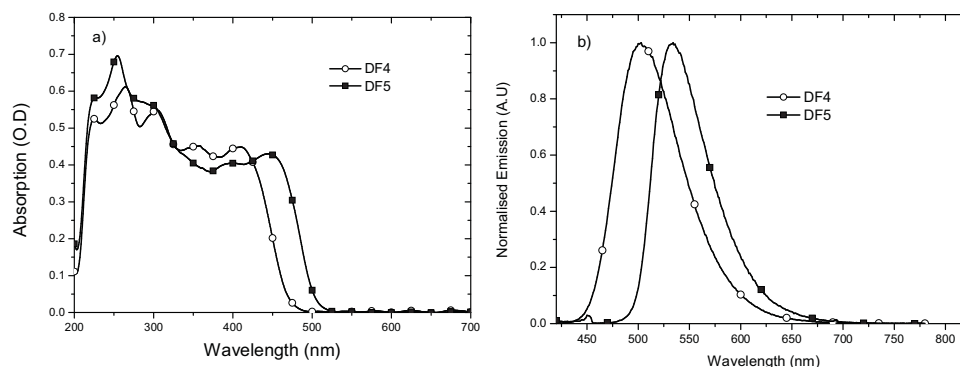
To further investigate the role of TF in increasing EQE in fluorescent OLEDs, anthracene core small molecules were synthesized, denoted as **DF1**, **DF4**, and **DF5**, as shown in **Figure 1**. Synthetic details of all members of this family are given in the Supporting Information. The delayed fluorescence (DF) of the parent crystalline anthracene has been observed and studied

Figure 2. a) Absorption spectra of emitters dispersed in a inert zeonex host. b) Emission of emitters dispersed in inert zeonex host.

**Table 1.** The quantum yields for the investigated emitter materials.

Material	Quantum Yield [%]
DF4	39 ± 3
DF4 in zeonex	70 ± 3
DF5	39 ± 5
DF5 in zeonex	80 ± 5

in toluene are given in the Supporting Information (Figure S1). **DF5** also shows the strongest green emission and both emitters display unstructured Gaussian like emission bands.

The measured quantum yields for both emitters are given in **Table 1**. The yields obtained clearly show that emission is high when self quenching (neat film case) is avoided by dilution of the emitter in an inert matrix (zeonex), although they do not reach 100%, the values of 0.70 ± 0.03 and 0.8 ± 0.05 are still high.

The fluorescence properties of these materials where further investigated by examining any solvatochromic behavior with **DF5** being dissolved in three different solvents of different polarity: toluene, chlorobenzene, and acetonitrile; the results are shown in **Figure 3**, with an excitation wavelength of 410 nm. It is seen that the fluorescence spectra bathochromically shifts quite strongly with increasing polarity of the solvent, indicative of an excited state (π to $\pi*$) transition with a degree of ground state charge transfer. This behavior indicates that the (excited state) excitons will also have charge transfer character, consistent with the nonsymmetric A-D-A structure of the molecule, and consistent with similar DA systems we have reported on in detail previously.[16] This behavior is found in **DF4** with similar magnitude but not in **DF1**.

Fluorescence decays and fits of the **DF5** measured in dilute toluene solution and zeonex thin film are shown in **Figure 4**. Emission was collected at three different emission wavelengths.
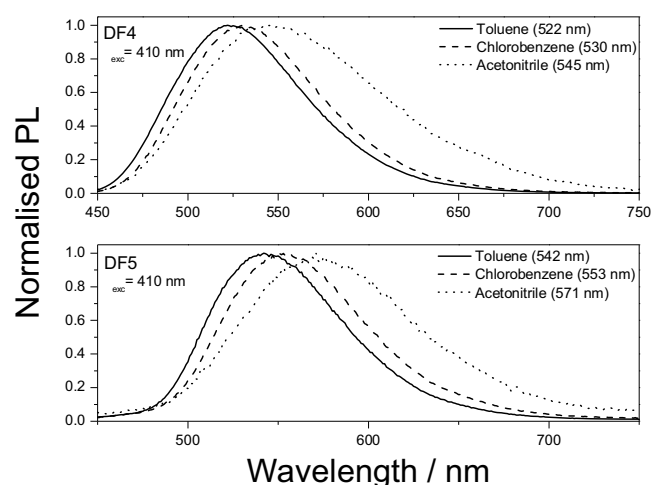
Figure 3. Solvatochromism of the emission of DF4 and DF5 in increasingly polar solvents. Emission peak wavelengths are given on the plots.

In solution, the most prominent decay has a lifetime of 2.20 ± 0.01 ns, with a fast decay of 15 ± 1 ps which is especially prominent on the blue edge. The fit also reveals a small amplitude decay component of 200 ± 0.01 ns. Emission collected on the blue edge of the emission bands show clear lifetime quenching. Given that the molecules display pronounced solvatochromism indicating intramolecular charge transfer (CT), the rapid decay on the blue edge of the emission spectrum indicates the evolution of the CT state with the rate of 2×10^{10} s^{-1}. The long lifetime and high PL quantum yield are indicative of a strongly coupled intramolecular CT excited state whereas the shorter lifetime could be interpreted as residual excitonic emission.[17] Emission decay for **DF4** in solution for comparison is given in the Supporting Information (Figure S2). In the zeonex host, Figure 4b, there is much less evidence of intramolecular charge transfer with only a small fast decay component on the blue edge with lifetime 4 ± 1 ps. The long (1.97 ± 0.01 ns) and shorter (0.48 ± 0.01 ns) decay components have roughly equal weighting in the decay. One could interpret this as the host matrix restricting molecular twisting so limiting the intramolecular CT.[18] Full fluorescence decay fitting data is given in **Table 2**.

Weak phosphorescence spectra for **DF4**, peaking at 1.75 eV and for **DF5** at 1.78 eV, were observed, as shown in **Figure 5**; these values are consistent with that of anthracene (1.85 eV) found in the literature[19,20] and confirmed by us, see the Supporting Information (Figure S3). The small decreases observed as the molecular conjugation length increases is consistent with the general saturation behavior of triplet energies in long conjugated systems.[21] The decay of the DF and PH of **DF4** and **DF5**, are quite distinct. For **DF4** the DF at room temperature has a lifetime of 4 μs but at low temperature (15 K) the lifetime extends to much longer times (600 μs), two orders of magnitude larger than the value at room temperature. The PH however remains independent of temperature with a lifetime of 3 μs at room temperature and 4 μs at low temperature. For **DF5** however, both the DF and PH remain temperature independent with values of DF lifetime of 1 μs and 2 μs for 15 K and room temperature, respectively. The PH for this molecule is estimated to be 4 μs at 15 K and 3 μs at room temperature. Although it is curious that there is such deviation between the two materials there are reports in the literature about the strange behavior of the temperature dependence of anthracene triplet decay. Siebrand et al. report unusual and long lifetimes of DF in anthracene believed to be due to triplet trapping at low temperature.[22] However, as the phosphorescence is so weak it is not possible to ascertain clear spectral shifts in the phosphorescence to indicate emission from free and trapped triplet excitons to support this model. To fully understand these effects, more extensive triplet dynamics studies will need to be made. This phenomenon could be the explanation of the large increase in the DF lifetime for **DF4** but no change in the PH lifetime. For the **DF5** where there is no change in either the PH or DF, this could be due to a lack of traps for the triplet states and thus remain temperature independent, as reported by Yokoi et al.[23] Given the very weak temperature dependence of the phosphorescence we can rule out E-type fluorescence[24] as the mechanism for generating the DF, consistent with the large exchange energy of these materials. In an effort to probe this further, the DF and phosphorescence kinetics were
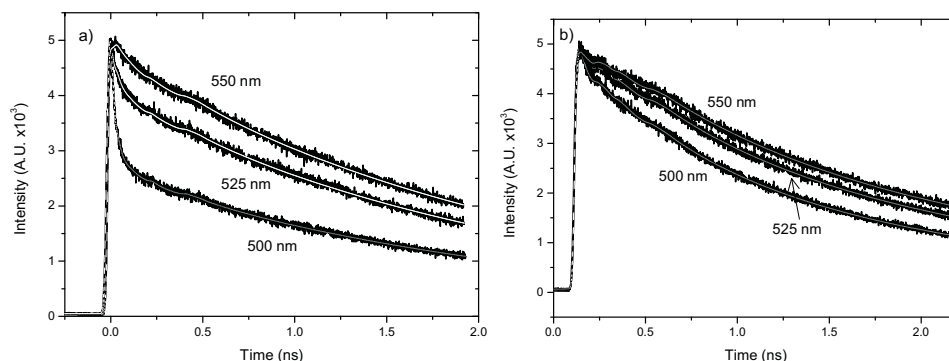
Figure 4. The singlet lifetime decay measured in solution for a) **DF5** in toluene solution and b) **DF5** in a zeonex host film. Emission is measured at three wavelengths related to the blue edge, peak, and red edge of the emission spectra, excited at 425 nm. White black segmented lines are exponential fits.

measured, see **Figure 6**. At room temperature, **DF4** shows fast triplet migration and rapid turn over from dispersive to non-dispersive hopping.[25] At low temperature (15 K), this turn over takes longer as expected and dispersive migration is very slow, which is consistent with triplet exciton trapping at low temperature in the amorphous film.

The T_1-T_n transition for **DF4** and **DF5** are shown in **Figure 7**, and in line with the very small differences in triplet exciton energy of the two, triplet absorption is observed at 654 nm (1.90 eV) for **DF4** and 685 nm (1.81 eV) for **DF5** (peak position). Given the T_1 energy for **DF4** and **DF5** was found to be 1.75 eV and 1.78 eV respectively (peak position), we have a criterion that for both **DF4** and **DF5**, $2T_1 \leq T_n$ (energy) on an absolute scale. This has important ramifications for the triplet fusion process, as will be discussed later.

For the simple device structure used here, the injecting energy barrier between the ITO anode and HOMO level of the DF dopants is lower than that of the host, whereas it is the opposite case for the cathode and LUMO interface. Holes are thus expected to inject into the dopant while electrons inject into the host. The excitons will be formed either on the host TPBi or the DF dopants, although with the doping concentration as large as 20% by rate, the charge carriers are more likely to be trapped and excitons formed directly on the dopants. Device characteristics curves are given in the Supporting Information (Figure S4). The current density increases for both **DF4** and **DF5** devices when the doping concentration increases from 10% to 20%, indicating that holes are transported through the dopants. At a current density of 0.7 mA/cm², the EQE of 10% doped **DF4** and **DF5** devices are ≈3% and ≈2%, respectively, which increases to ≈5.0% and ≈4.5% when the doping concentration increases to 20% due to the better charge carrier balance. In comparison, similar devices made with 20% **DF1** doping, which have no hole
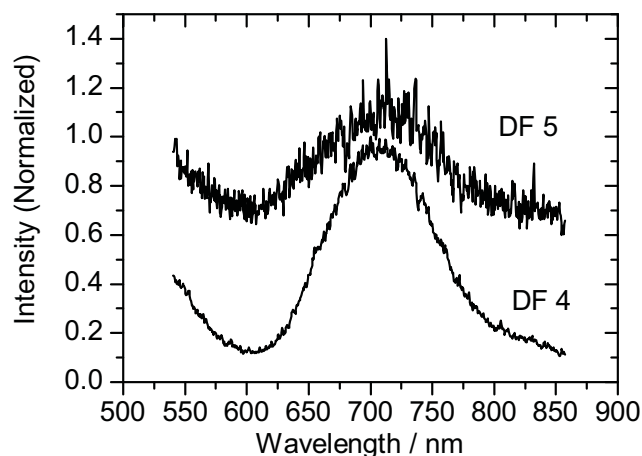

Figure 5. Normalized phosphorescence spectra of DF4 and DF5 films. The spectra were recorded with a 4 and 3.2 μs delay after excitation for the DF4 and DF5 films, respectively. Excitation was at 355 nm.

transporting end caps, are very poor (EQE 0.9%, 0.8 lm/W and 100 cd/m² @ 4.7 mA/cm²). The **DF4** devices surpass the 5% limit according to Equation (1), which indicates that in these devices more than 25% of the singlet production is contributing to the electroluminescence. Furthermore, 5% is deduced based on the assumption that the fluorescence quantum yield (FLQY) is 100%. The PLQY of **DF4** and **DF5** films measured 0.70 ± 0.03 and 0.80 ± 0.05 when doped in zeonex. Thus, in the case of **DF5**, the upper limit of Equation 1, which shows that in these simple architectures the theoretical maximum EQE value is exceeded by a large extent. It is clear that the diphenylamine end groups are responsible for the high charge mobility in the emission layers containing the dopants increasing mobility.

Table 2. Fluorescence lifetime fitting parameters from DF5 in both dilute toluene solution and in zeonex host.

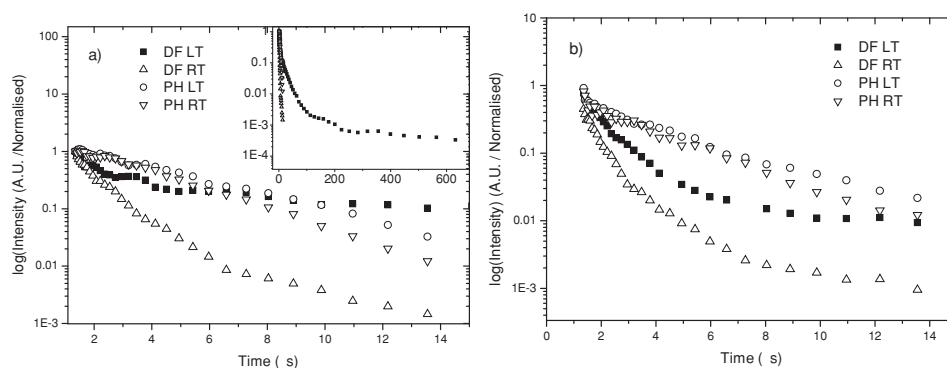|	A_1	τ_1 [ns]	A_2	τ_2 [ns]	A_3	τ_3 [ns]
DF5 in toluene solution	0.74 ± 0.01	2.2 ± 0.01	0.18 ± 0.01	0.2 ± 0.01	0.88 ± 0.04	0.015 ± 0.001
DF5 in zeonex film	0.59 ± 0.01	1.97 ± 0.01	0.49 ± 0.01	0.48 ± 0.01	0.29 ± 0.04	0.04 ± 0.001

Figure 6. Delay Fluorescence (DF) and Phosphorescence (PH) decay measured at room temperature (RT) and 15 K (LT) for a) DF4 and b) DF5.
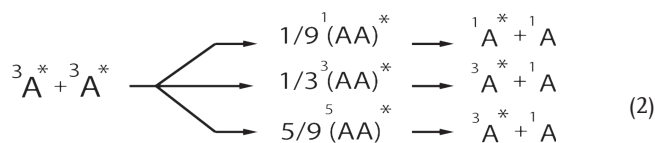
To further improve charge carrier balance, an extra thin layer (5 nm) of **DF5** adjacent to the anode was added to block the electron current while maintaining the total thickness of the OLED at 120 nm; (Dev7, Supporting Information). In these double-layered devices, an improved EQE of ≈5.5% was obtained. The EBL was optimized in thickness, whilst maintaining a total OLED thickness of 120 nm. **Figure 8** shows the device characteristics for Dev1 with a 10-nm-thick **DF4** electron-blocking-layer (EBL) and 110 nm of 20% **DF4** doped TPBi light-emitting-layer, and for Dev2 with an EBL of 15 nm. A maximum EQE value of ≈6%, 20 cd/A (compared to the predicted theoretical maximum value of ≈3.55%) was achieved, nearly twice the expected theoretical maximum device performance. We also note that the simple two layer device structure also yields stable efficiency through larger current density and high brightness. EL spectra for various device configurations used here are given in **Figure 9**.

This excellent device performance is achieved by successfully forming the excitons on the dopants in the heavily doped region and confining the 75% of triplet excitons in the doped region by the high triplet energy well of the TPBi. This increases the probability that two triplets annihilate. If the triplet-triplet annihilation (TTA) process is faster than the nonradiative monomolecular decay of triplets, the delayed fluorescence can be very efficient as is observed in these DF devices. To verify this, transient EL measurements were also conducted on the DF devices as seen in **Figure 10**. In the case of the **DF4** (Dev2), the results

show that the delayed electroluminescence contributes ca. 59% of the total EL signal (at device turn off).

3. Discussion

Classically the triplet-triplet annihilation process can be understood following Equation 1 as first proposed by Jortner et al.:[26]

$$^3A^* + {}^3A^* \begin{cases} 1/9\,{}^1(AA)^* \longrightarrow {}^1A^* + {}^1A \\ 1/3\,{}^3(AA)^* \longrightarrow {}^3A^* + {}^1A \\ 5/9\,{}^5(AA)^* \longrightarrow {}^3A^* + {}^1A \end{cases} \tag{2}$$

Here, two triplet excitons, upon colliding, can form an intermediate state which has 1 of 9 possible spin configurations, having 1/9 singlet character, 1/3 triplet character, and 5/9 quintuplet character. The quintuplet state has two spins on one site and so is highly energetically unstable. For C_{60}, it has been calculated that a quintet state would physically break a C–C bond[27] and calculations for DPA, diphenylanthracene, indicate that the quintet state is too energetic to form from two triplets.[20,28] Thus, we assume that quintuplets play no part here and so the total singlet production from annihilation or triplet fusion yield will be
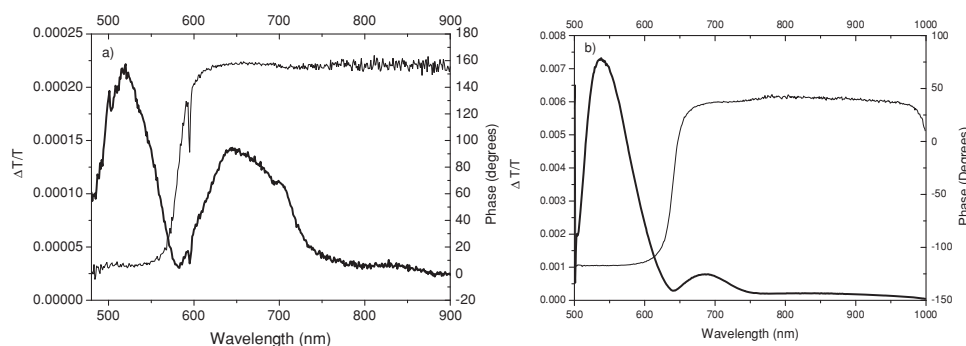

Figure 7. The T_1-T_n absorption for a) DF4 and b) DF5 (in zeonex host films) at 15 K. Thick black straight line is magnitude, thin black line is phase of the measured photoinduced absorption. Signal at 0° phase is fluorescence, that at 180° phase is induced absorption arising from the T_1-T_n absorption.
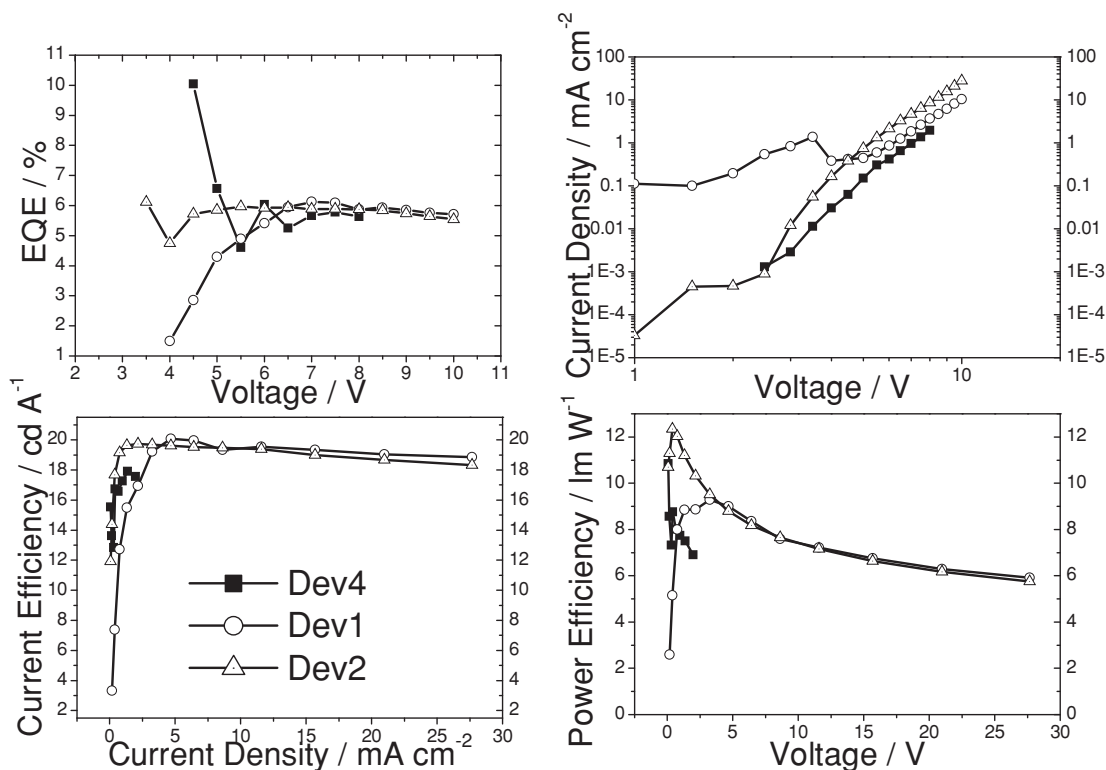
**ADVANCED
FUNCTIONAL
MATERIALS**

www.afm-journal.de

*Materials
Views*

www.MaterialsViews.com

Figure 8. Device parameters and efficiencies measured for both types of device using the **DF4** EBL compared to a single layer device without the EBL. Device structures are given in the Experimental Section. For Dev1 and Dev2, brightness levels of 5000 cd/m² were measured at 29 mA/cm² at 10 V. A brightness of 1000 cd/m² was attained at a 4.8 V bias.

$$\sum_{N=0}^{\infty} \frac{13^n}{18^{n+1}} = 0.2 \qquad (3)$$

This accounts for multiple annihilation and fusions steps until the triplet population is exhausted. However, as we have shown,

in these new anthracene containing emitters, $2T_1 \leq T_n$ which means two triplet excitons do not have enough energy to create a single triplet in its excited (T_n) state. In this particular scenario, the two triplets cannot form the triplet intermediate pair state on energetic grounds and so the only energetically possible TTA
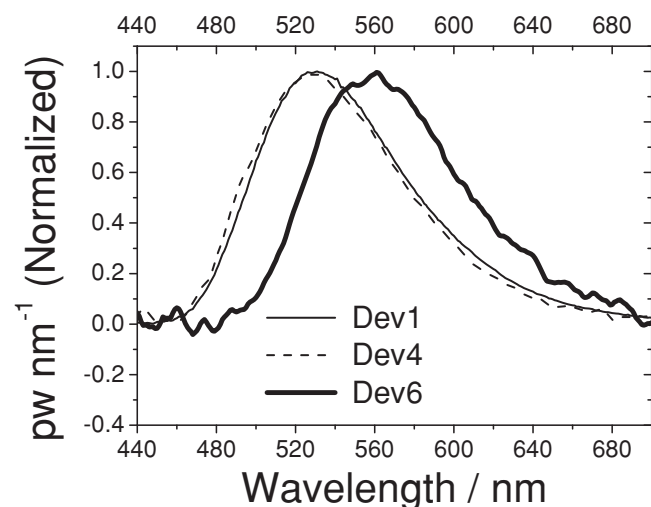

Figure 9. Electroluminescence spectra for various device configurations used through these studies. Device structures are given in the Experimental Section and the Supporting Information.
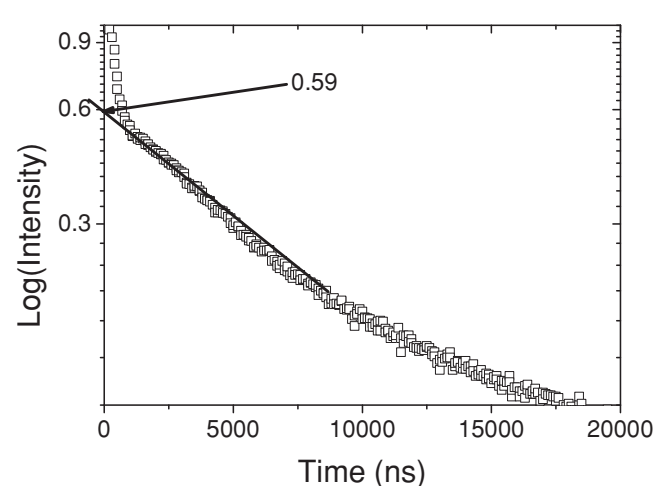

Figure 10. Delay electroluminescence decay measured after the device turned off using gated iCCD detection to record the transient electroluminescence decay from a DEV2 device. The intercept of the DF at time zero (turn off) is indicated on the graph.

www.MaterialsViews.com

ADVANCED
FUNCTIONAL
MATERIALS
www.afm-journal.de

FULL PAPER

channel is the singlet TF channel. In this case, if all triplets annihilate, a total singlet production yield of 0.5 will result.

Calculating the maximum contribution of direct singlet and triplet fusion to the electroluminescence signal of a **DF4** Dev2 device, we see that we have the following contributions; singlet $\varphi_S \times \varphi_{fl} = 0.25 \times 0.7 = 0.175$, triplet, $\varphi_T \times \varphi_{TF} \times \varphi_{fl} = 0.75 \times 0.5 \times 0.7 = 0.26$, thus the ratio of singlet to TF signal is 67%. From Figure 10 we see that the delayed electroluminescent signal from triplet fusion is approximately 59%. Clearly not all triplets are able to annihilate and contribute to TF, as can be seen in Figure 10, there is a weak tail which shows a much slower triplet TF process which we believe occurs as triplet migration changes from nondispersive to dispersive hopping. Also, given the rather broad spectral features (wide DOS), indicative of high disorder, there is still some overlap between $2T_1$ and T_n so that some triplet triplet encounters can still create a T_n state. More work to fully elucidate the whole photophysics of the triplet annihilation processes clearly needs to be made in order to fully address these subtle points. It is clear that the TF contribution measured here is approaching the maximum, when the TF yield (during the annihilation process) reaches 0.5. These devices show a total singlet production yield of 0.58, a consequence of the finding that in these new materials $2T_1 \leq T_n$.

4. Conclusions

Three fluorescent emitters based on anthracene were synthesized and 4 highly efficient simple-structure OLEDs were successfully fabricated using these materials as dopants and TPBi as the host. These emitters have intramolecular charge transfer character excited states with high PLQY. Although the predicted upper limit of the EQE of the fluorescent OLEDs is 5%, in optimized doping concentration (20% by rate) devices, the EQE of **DF4** devices reached 5.5% (8 lm/W and 100 cd/m^2 @ 0.7 mA/cm^2). By adding an additional EBL, the EQE of **DF4** devices could be improved further to 6% (11.2 lm/W and 260 cd/m^2 @ 1.3 mA/cm^2). This compares to a theoretical maximum EQE for a **DF4** device of 3.55%, taking into account the PLQY of the emitter. The enhancement above the theoretical maximum EQE was shown to be due to a high contribution from delayed fluorescence arising from TF. Measurement of first and second triplet energies confirmed that in these emitters $2T_1 \leq T_n$ permitting TF efficiencies to reach 0.5. Transient delayed electroluminescence measurements show that TF is contributing 59% of the total EL signal, very close to the maximum of 67% for the emitter **DF4** clearly indicative of near 0.5 TF singlet yield. These findings are the first to confirm the validity of possible 0.5 yield for the TF process as determined from an OLED device. Finally, the tri-benzenamine is believed to be an important factor for the very high efficiency of these simple fluorescence devices, both increasing mobility and creating a CT emitter state, which provides the hint for the future material development for highly efficient blue delayed fluorescence materials. Given a 0.5 TF yield and a singlet PLQY of 1, the maximum internal EQE attainable will be 62.5%. It is clear that even with a very simple OLED structure, highly efficient fluorescent devices can be realized.

5. Experimental Details

Quantum yields were measured using an integrating sphere in a Jobin-Yvon fluoromax spectrometer in the standard setup using the method as described by Palsson and Monkman.[29] The singlet fluorescent lifetime measurements were made using time-correlated single photon counting as previously described.[30]

Decay measurements of both PH and DF were measured using an ESKPLA SL312 Nd:YAG laser and a gated iCCD (Stanford Computer Optics2 4Picos) to collect the data, as described in references.[31] The T_1-T_n absorption was measured using a Quasi-CW Pump Probe with excitation from a 50 mW, 405 nm laser diode directly modulated by the reference output of the lock-in amplifier, a focused Xe arc lamp was used as a probe source with the detection post-monochromation being made by Si and GaAs detectors and lock-in amplification.[32]

Instead of the thick multilayered device fabricated by Kondakov,[28] initial single-layered devices, inspired by the structure used by Liu et al. in their work on phosphorescent iridium metal complex,[33] were fabricated on the indium-tin-oxide (ITO) coated glass substrates purchased from Visiontek with sheet resistance of 15 Ω/sq and ITO thickness of 150 nm. They were patterned so that the OLED devices will have the pixel size of 5 mm by 6 mm. The standard cleaning process was then applied to the substrates: 10 min of acetone followed by 10 min of isopropyl alcohol washed in an ultrasonic bath, and finally cleaned with the oxygen plasma. The small molecule and cathode layers were thermally evaporated using a Kurt J. Lesker Spectros II deposition system under the vacuum condition of 5×10^{-6} mbar. To improve charge carrier balance, further devices were fabricated by inserting an extra thin layer (5 nm) of pure **DF5** adjacent to the anode to block the possible leakage of the electron current while maintaining the total thickness of the OLED to be 120 nm. Based on this improved device structure, better optimized devices for charge balance (but not for optimal optical performance of the effective cavity) were fabricated with DF4 as the dopant and electron blocking material:

Dev1. Glass/ITO/DF4 (10 nm)/TPBi (2 Å/s):DF4 (0.4 Å/s) (110 nm)/ LiF (1 nm)/Al (100 nm).
Dev2. Glass/ITO/DF4 (15 nm)/TPBi (2 Å/s):DF4 (0.4 Å/s) (105 nm)/ LiF (1 nm)/Al (100 nm).

Device current-voltage (*I*–*V*) characteristics and the emission intensities were measured in a calibrated integrating sphere and the data acquisition was controlled using a home-written NI LabView program which controlled the Agilent Technologies 6632B power supply. The electroluminescence (EL) spectra were measured using an Ocean Optics USB 4000 CCD spectrometer supplied with 400 μm UV-vis fiber optics. Transient decay of electroluminescence is recorded using a fast voltage source (HP 8114A) to turn the device off within 10 ns. The emission from the device is recorded using the same gated iCCD based detection system as described above for phosphorescence and DF measurements.[11]

Supporting Information

Supporting Information is available from the Wiley Online Library or from the author.

Acknowledgements

FULL PAPER

[1] M. A. Baldo, S. Lamansky, P. E. Burrows, M. E. Thompson, S. R. Forrest, *Appl. Phys. Lett.* **1999**, *75*, 4.

[2] C. Adachi, M. A. Baldo, S. R. Forrest, S. Lamansky, M. E. Thompson, R. C. Kwong, *Appl. Phys. Lett.* **2001**, *78*, 1622.

[3] M. A. Baldo, D. F. O'Brien, Y. You, A. Shoustikov, S. Sibley, M. E. Thompson, S. R. Forrest, *Nature* **1998**, *395*, 151.

[4] Y. J. Li, H. Sasabe, S. J. Su, D. Tanaka, T. Takeda, Y. J. Pu, J. Kido, *Chem. Lett.* **2010**, *39*, 140.

[5] S. O. Jeon, J. Y. Lee, *Mater. Chem. Phys.* **2011**, *127*, 300.

[6] N. Chopra, J. Lee, J. G. Xue, F. So, *IEEE Trans. Electron Devices* **2010**, *57*, 101.

[7] S. Mladenovski, K. Neyts, D. Pavicic, A. Werner, C. Rothe, *Opt. Express* **2009**, *17*, 7562.

[8] V. Sivasubramaniam, F. Brodkorb, S. Hanning, H. P. Loebl, V. van Elsbergen, H. Boerner, U. Scherf, M. Kreyenschmidt, *J. Fluorine Chem.* **2009**, *130*, 640.

[9] V. Jankus, A. P. Monkman, *Adv. Funct. Mater.* **2011**, *21*, 3350.

[10] D. Y. Kondakov, T. D. Pawlik, T. K. Hatwar, J. P. Spindler, *J. Appl. Phys* **2009**, 106.

[11] S. Sinha, A. P. Monkman, *Appl. Phys. Lett.* **2003**, *82*, 4651.

[12] S. Sinha, C. Rothe, R. Guntner, U. Scherf, A. P. Monkman, *Phys. Rev. Lett.* **2003**, *90*, 127402.

[13] S. M. King, M. Cass, M. Pintani, C. Coward, F. B. Dias, A. P. Monkman, M. Roberts, *J. Appl. Phys.* **2011**, 109.

[14] a) R. G. Kepler, J. C. Caris, P. Avakian, E. Abramson, *Phys. Rev. Lett.* **1963**, *10*, 400; b) W. L. Peticolas, J. P. Goldsborough, K. E. Rieckhoff, *Phys. Rev. Lett.* **1963**, *10*, 43.

[15] a) K. H. Kim, J. Y. Lee, T. J. Park, W. S. Jeon, G. P. Kennedy, J. H. Kwon, *Synth. Met.* **2010**, *160*, 631; b) G. Y. Ding, W. L. Jiang, G. D. Wang, Q. A. Han, X. Chang, in *New Materials and Advanced Materials, Pts 1*, Vol. *152* (Eds: Z Jiang, J. Han and X. Liu), Trans Tech Publications Ltd, Stafa-Zurich **2011**, p. 687.

[16] a) S. M. King, I. I. Perepichka, I. F. Perepichka, F. B. Dias, M. R. Bryce, A. P. Monkman, *Adv. Funct. Mater.* **2009**, *19*, 586; b) F. B. Dias, S. King, A. P. Monkman, I. I. Perepichka, M. A. Kryuchkov, I. F. Perepichka, M. R. Bryce, *J. Phys. Chem. B* **2008**, *112*, 6557.

[17] F. Dias, S. PollocK, G. Hedley, L. O. Palsson, A. P. Monkman, I. I. Perepichka, I. F. Perepichka, M. Tavasli, M. R. Bryce, *J. Phys. Chem. B* **2006**, *110*, 19329.

[18] K. C. Moss, K. N. Bourdakos, V. Bhalla, K. T. Kamtekar, M. R. Bryce, M. A. Fox, H. L. Vaughan, F. B. Dias, A. P. Monkman, *J. Org. Chem.* **2010**, *75*, 6771.

[19] S. Murov, I. Charmichael, G. L. Hug, *Handbook of Photochemistry*, Dekker Inc., NY **1993**.

[20] G. C. Smith, *Phys. Rev.* **1968**, *166*, 839.

[21] A. P. Monkman, H. D. Burrows, I. Hamblett, S. Navarathnam, M. Svensson, M. R. Andersson, *J. Chem. Phys.* **2001**, *115*, 9046.

[22] W. Siebrand, *J. Chem. Phys.* **1965**, 42.

[23] K. Yokoi, Y. Ohba, *Jpn. J. Appl. Phys.* **1980**, *19*, 1655.

[24] a) G. N. Lewis, D. Lipkin, T. T. Magel, *J. Am. Chem. Soc.* **1941**, *63*, 3005; b) A. Endo, K. Sato, K. Yoshimura, T. Kai, A. Kawada, H. Miyazaki, C. Adachi, *Appl. Phys. Lett.* **2011**, 98.

[25] a) C. Rothe, A. P. Monkman, *Phys. Rev. B* **2003**, *68*, 075208; b) C. Rothe, A. Monkman, *Phys. Rev. B* **2002**, *65*, 073201.

[26] J. Jortner, S. A. Rice, J. L. Katz, *J. Chem. Phys.* **1965**, *42*, 309.

[27] R. Froese, K. Morokuma, *Chem. Phys. Lett.* **1999**, *305*, 419.

[28] D. Y. Kondakov, *J. Soc. Inf. Disp.* **2009**, *17*, 137.

[29] a) L. O. Palsson, A. P. Monkman, *Adv. Mater.* **2002**, *14*, 757; b) L. Porres, A. Holland, L. O. Palsson, A. P. Monkman, C. Kemp, A. Beeby, *J. Fluoresc.* **2006**, *16*, 267.

[30] S. I. Hintschich, C. Rothe, S. Sinha, A. P. Monkman, P. S. de Freitas, U. Scherf, *J. Chem. Phys.* **2003**, *119*, 12017.

[31] a) C. Rothe, R. Guentner, U. Scherf, A. P. Monkman, *J. Chem. Phys.* **2001**, *115*, 9557; b) V. Jankus, C. Winscom, A. P. Monkman, *J. Phys.: Condens. Matter* **2010**, *22*, 185802.

[32] A. Monkman, C. Rothe, S. King, F. Dias, in *Polyfluorenes* Vol. *212*, (Eds: U. Scherf, D. Neher), Springer, Berlin **2008**, p. 187.

[33] Z. Liu, M. G. Helander, Z. Wang, Z. Lu, *Org. Electron.* **2009**, *10*, 1146.